EPITHELIAL IMPEDANCE ANALYSIS IN EXPERIMENTALLY INDUCED COLON CANCER

RICHARD J. DAVIES, RENAH JOSEPH, DAVID KAPLAN, ROBERT D. JUNCOSA, CIRO PEMPINELLO, HORACIO ASBUN, AND MARC M. SEDWITZ

The Department of Surgery, University of California, San Diego, California 92103; and Veterans Administration Medical Center, La Jolla, California 92093

ABSTRACT Epithelial impedance analysis was used to measure the alterations in resistance of the large bowel in a murine model of large bowel cancer. The technique was able to resolve the epithelial resistance from the total resistance of the bowel wall. A progressive decrease in resistance of the bowel epithelium occurs during carcinogenesis induced with dimethyhydrazine. About a 21% decrease in epithelial resistance from 22.0 ± 1.3 $\Omega \cdot cm^{-2}$ to 17.5 ± 1.1 $\Omega\, cm^{-2}$ ($p < 0.025$) was observed after 20 wk of carcinogen administration. The sensitivity of the technique in detecting altered epithelial resistance in premalignant bowel mucosa was improved by examining the impedance profile in a sodium-free Ringer's solution where the epithelium of control colons had a resistance of 24.4 ± 1.8 $\Omega \cdot cm^{-2}$ compared with 19.0 ± 1.1 $\Omega \cdot cm^{-2}$ ($p < 0.02$) in colons from animals treated for only 4 wk with the carcinogen. Epithelial impedance analysis would seem to be a sensitive technique capable of identifying changes in the electrical properties or the large bowel early in disease states.

INTRODUCTION

Cell surface changes are of fundamental importance in the regulation of growth, with many of the earliest events in growth stimulation appearing to be mediated at the cell membrane. Furthermore, the binding of growth factors promotes the generation of early signals at the cell surface or within the cytosol (1). Within minutes the mitogenic signal is propagated to the nucleus. These initial events are followed in parallel sequence by multiple molecular and cellular responses which eventually converge into a final path leading to the synthesis of DNA and cell division (2).

It is likely that early events at the cell surface will provide clues to primary regulatory mechanisms. Two of the earliest events in signal transduction at the cell surface are clustering of specific receptor molecules in the plane of the membrane (3–5) and the rapid induction of ion fluxes through the membrane (6–8). These two events may be linked since it has been suggested that certain receptor molecules are potential ion channel formers (9). Other changes also occur with both growth stimulation and malignant transformation, such as alterations in the tight junction between cells and in the glycocalyx skeleton covering the plasma membrane surface (10, 11). Much of the investigation of these phenomena has involved immunologic and cell biologic approaches, although since these early changes involve the cell surface, electrophysiologic methodologies may provide important insight into growth regulation and the loss of regulation involved in transformation.

Most of the commonly occurring malignancies in man are of epithelial origin, whereas tumors of endodermal or mesodermal origin are rare (12). Epithelia function primarily to transport ions and water, often against considerable electrochemcial gradients from lumen to blood stream or in the opposite direction (13). Two approaches are used to study transport mechanisms. The first is to measure unidirectional fluxes of ions with radioisotopes. The second method involves measuring electrical properties of tissue, most notably transepithelial potentials, short-circuit currents, and membrane conductances. Biological membranes exhibit a remarkably constant electrical specific capacitance of ~1 $\mu F/cm^2$ (14, 15). The total capacitance of a membrane is directly proportional to the membrane area and, therefore, a determination of this capacitance can be used as a measure of the membrane area (using 1 $\mu F/cm^2$ as the proportionality constant). The resistance of a membrane, determined mainly by the ionic permeability properties of that membrane, coupled with the capacitance, forms a parallel resistor-capacitor (RC) circuit with a characteristic time constant equal to $R \times C$ (see Fig. 4). Therefore it is possible to construct an electrical equivalent circuit analog of the epithelium made up of resistors and capacitors. The characterization of the electrical circuit may be accomplished by measuring the electrical impedance, which is simply the ratio of the measured voltage to a constant-applied sinusoidal current at a given frequency. At each frequency two quantities were measured: the ratio

Address reprint requests to Dr. Richard J. Davies, Division of Surgical Oncology, UCSD Medical Center, H-891-B, 225 Dickinson St., San Diego, CA 92103.

of the magnitudes of the applied to the measured voltage and the normalized time delay of the voltage sinusoid compared with the current sinusoid (the phase angle). This relationship can then be represented as a Nyquist plot, and the impedance characteristics of the epithelium may be estimated.

The purpose of this study was to use impedance analysis to characterize the electrical properties of colonic epithelium in a murine model of colon cancer, since these properties may provide insight into growth regulatory mechanisms in large bowel cancer. Furthermore, the technique may be useful in evaluating the electrical properties of epithelia in health and disease.

MATERIALS AND METHODS

Nonfasting adult female CF_1 mice (Charles River Breeding Laboratories, Inc., Wilmington, MA) weighing between 19 and 21 g were used in all experiments, and were kept under identical conditions of cyclic 12 h light and dark. Regular Purina Chow (Ralston Purina Co., St. Louis, Mo) and water were allowed ad libitum.

The carcinogen 1,2 dimethylhydrazine (DMH) (Aldrich Chemical Co., Inc., Milwaukee, WI) was freshly prepared on the day of injection and dissolved in 0.9% saline and injected subcutaneously into the groin in a dose of 20 mg/kg weekly for 4, 14, or 20 wk in a negative flow hood. Another group was similarly injected with 5-fluorouracil (35 mg/kg) weekly for 4 wk. Control animals were subcutaneously injected with an identical volume of 0.9% saline. All animals receiving the carcinogen were kept in a negative flow hood for 12 h to prevent atmospheric contamination.

One week after their last injection animals were killed using cervical dislocation and the colon was removed and rinsed with iced standard Ringer's solution. Since preliminary studies failed to demonstrate any difference in stability of the tissue whether or not the seromuscular layer was stripped, all experiments were performed on pieces of colon containing all layers, including the mucosa. Each distal section of colon was mounted within 10 min of the killing in an acrylic chamber (area, 0.28 cm^2) and bathed on the mucosal and serosal sides with equal volumes of standard Ringer's or sodium-free Ringer's solutions at 37°C continuously oxygenated with 95% O_2-5% CO_2, maintained at a pH of 7.4, and circulated using a bubble-lift mechanism.

The Ringer's solution contained (in millimolars) Na, 140; K, 5.2; Ca, 1.2; Mg, 1.2; HCO_3, 25; HPO_4, 2.4; H_2PO_4, 0.4; Cl, 119.8; and glucose, 10. In the sodium-free Ringer's solution choline replaced sodium in equimolar concentrations.

Fig. 1 illustrates the circuitry of the measuring equipment. A signal generator was used to excite the colon with a sine wave signal of adjustable frequency. The resultant voltage drop caused by the colon sample was compared with the voltage drop across an external adjustable load consisting of a parallel combination of a resistor and capacitor. When the comparison of these two signals yielded a "zero error," the tissue impedance was considered to be that of the external load. A constant voltage of 40 mV was used to stimulate the tissue, and since the measured resistance was a function of frequency, the current varied between 60 and 110 μA. At the greatest current applied the tissue was noted to behave as an ohmic resistor, with the relationship of voltage to current remaining linear at each frequency. The sine wave signal was used at 12 different frequencies: 20, 50, 70, 100, 200, 500, 700, 1,000, 2,000, 5,000, 7,000, and 10,000 Hz. The measured capacitance of the chamber and leads was <100 pF. Differences in impedance due to the chamber when compared with the external adjustable load were balanced out during the calibration procedure, and since the calibration signal was applied to both "R_1/C_1" and "R_2/C_2," errors due to internal sources were nulled. Further information describing the measuring equipment is given in Appendix I.

Stability of the tissue was noted for 150 min, although a slow decay in resistance and capacitance was noted over time. Therefore all experiments were completed within 30 min and were performed under steady state conditions 10 min after mounting the tissue in a modified Ussing chamber.

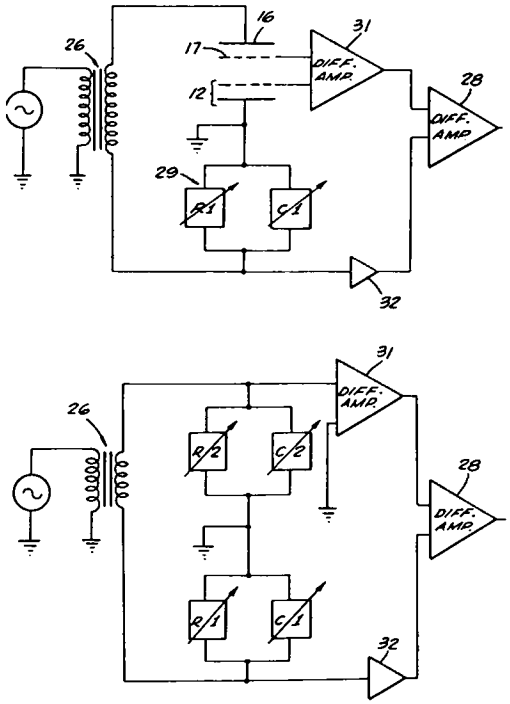

FIGURE 1 Circuit diagram of the two-stage impedance measurement apparatus, which is described in Appendix I.

Fig. 2 illustrates a typical Nyquist plot where capacitive reactance was plotted against resistance. Using a computer-generated curve fit analysis (Labtech Notebook, Laboratory Technologies Corp., Wilmington, MA) R_∞ (the resistance of the tissue at infinite frequency) R_o, (the resistance of the tissue at zero frequency) R_c, (the characteristic resistance that lays on the x-axis midway between R_o and R_∞), and the reactance (defined as the maximum capacitive reactance of the tissue) were estimated. Epithelial resistance (R_p) was defined as the difference between R_o and R_∞. From these four parameters simple trigonometry was used to derive the phase angle (ϕ), the suppression of the impedance locus (x), the radius of the

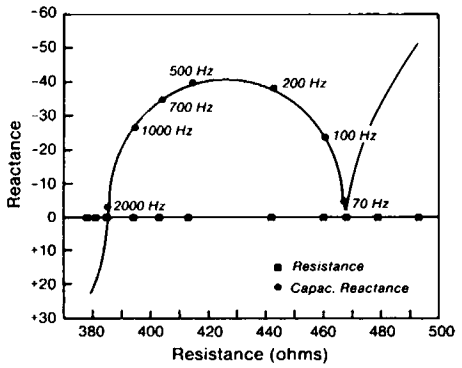

FIGURE 2 A typical impedance profile derived from the distal colon of CF_1 mouse. The reactance is plotted against resistance at different frequencies. Frequency values are given in hertz (Hz) and reactance and resistance in ohms. The derivation of the plot is discussed in detail in Appendix II.

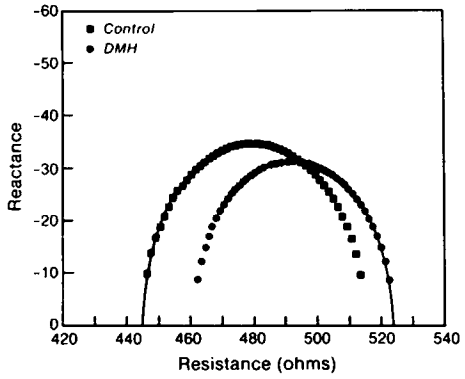

FIGURE 3 Summary Nyquist plots for the distal colon comparing 20-wk control animals (■) and 20-wk DMH-treated animals (●); otherwise same as Fig. 2. All observations are the mean of 10 control and 11 DMH-treated animals.

impedance plot (r), the characteristic frequency F_c (the frequency of the tissue at maximum capacitive reactance which coincides with the characteristic resistance R_c), the characteristic capacitance Cap_c (the capacitance of the tissue at maximum capacitive reactance), the time constant T ($R_c \cdot Cap_c$), and the angular frequency (w). Further information is included in Appendix II.

RESULTS

Fig. 3 illustrates the summary Nyquist plots for distal colon derived from saline-treated controls superimposed upon normal appearing distal colons derived from DMH-treated animals.

Table I summarizes the impedance characteristics of the control group after 20 wk of saline injections compared with the carcinogen-treated animals, which were treated for 20 wk. A significant increase in R_∞ was noted, suggesting an increase in the electrical resistance of the underlying muscle layer and serosa after 20 wk of DMH treatment; however, the epithelial resistance was significantly decreased by ~21% in the DMH-treated group.

The capacitive reactance and phase angle were significantly decreased in the DMH-treated animals. The characteristic resistance was significantly increased after DMH treatment, but characteristic frequency was significantly decreased. The impedance locus elevation decreased after DMH treatment. Although characteristic capacitance was somewhat higher, this did not reach statistical significance. It was noted that the capacitance of the tissue measured at low frequencies (20–100 Hz) was significantly lower in DMH-treated animals than in controls (data not shown).

Table II summarizes the impedance characteristics of distal colon after 4 wk of treatment with saline, DMH, or 5-fluorouracil (5-FU). DMH treatment significantly increased R_∞, as was observed after 20 wk of treatment; however, all the other parameters remained unaltered after only four treatments.

The nonspecific cytotoxic agent 5-FU caused significant increases in R_∞, R_0, and R_c. The increase in R_0 exceeded the increase in R_∞, resulting in an increase in epithelial resistance by ~11%. The characteristic frequency and angular frequency were increased significantly, although the time constant was significantly decreased.

Table III demonstrates the influence of 14 wk of saline or DMH-treatment on the impedance profile when measured in standard Ringer's solution. Epithelial resistance in DMH animals was decreased at 14 wk by 16%, similar to the changes observed at 20 wk although not by the same amount. Reactance, phase angle, and impedance locus elevation were reduced significantly and characteristic capacitance was increased.

Table IV demonstrates the influence of sodium removal on the impedance profile by mounting distal colons from

TABLE I
EPITHELIAL IMPEDANCE ANALYSIS CF_1 MOUSE DISTAL COLON

	R_0	R_∞	R_c	Reactance	R_p	Phase (ϕ)	x	r	F_c	T	w	Cap_c
	Ω	Ω	Ω	Ω	Ω · cm^{-2}	*rad*			*Hz*	*s*	*rad/s*	$\mu F \cdot cm^{-2}$
Control 20 wk (standard ringers)												
Mean	505.7	427.1	466.4	39.3	22.0	8.4E-2	9.0E-3	39.3	468.1	3.4E-4	2941.1	16.0
SE	8.2	5.7	6.7	2.4	1.3	4.6E-3	1.7E-3	2.4	6.7	5.0E-6	42.3	1.2
No.	10	10	10	10	10	10	10	10	10	10	10	10
DMH-treated 20 wk (standard ringers)												
Mean	523.5	461.0	492.3	31.2	17.5	6.4E-2	−1.8E-3	31.2	493.3	3.2E-4	3099.5	19.0
SE	8.0	9.4	8.5	2.0	1.1	4.8E-3	6.1E-3	2.0	8.4	5.5E-6	52.8	1.2
No.	11	11	11	11	11	11	11	11	11	11	11	11
p value	NS	0.01	0.05	0.025	0.025	0.01	0.025	0.025	0.02	0.02	0.02	NS

All results are expressed as mean ± SEM, p-value is derived from the unpaired Student's t-test comparing experimental samples with controls. No. denotes number of animals; R_0 is the resistance at zero frequency in ohms; R_∞ is the resistance at infinite frequency in ohms, R_c is the characteristic resistance in ohms; R_p is the epithelial resistance corrected for area in ohms · cm^{-2}; phase ϕ is the phase angle in radians; x is the deviation of the impedance locus from the x-axis, with a positive value indicating elevation and a negative value, suppression; r is the radius of the impedance profile; F_c is the characteristic frequency in hertz; T is the time constant in seconds, w is the time constant in radians/s; and Cap_c is the capacitance at the characteristic frequency and resistance in microfarads · cm^{-2}.

TABLE II
EPITHELIAL IMPEDANCE ANALYSIS CF_1 MOUSE DISTAL COLON

	R_0	R_∞	R_c	Reactance	R_p	Phase (ϕ)	x	r	F_c	T	w	Cap_c
	Ω	Ω	Ω	Ω	Ω · cm^{-2}	*rad*			*Hz*	*s*	*rad/s*	$\mu F \cdot cm^{-2}$
Control 4 wk (standard ringers)												
Mean	472.4	384.0	428.2	44.2	24.7	1E-1	4.6E-3	44.2	430.7	3.7E-4	2706.2	17.0
SE	11.4	6.1	7.7	4.8	2.7	9.6E-3	3.0E-3	4.8	8.1	6.8E-6	50.7	1.7
No.	11	11	11	11	11	11	11	11	11	11	11	11
DMH-treated 4 wk (standard ringers)												
Mean	478.4	407.0	440.2	38.2	21.4	8.6E-3	2.0E-3	38.2	441.9	3.6E-4	2776.4	18.0
SE	11.9	5.8	9.4	2.8	1.6	4.9E-3	3.7E-3	2.9	9.6	8.1E-6	60.4	1.8
No.	10	9	10	10	10	10	10	10	10	10	10	10
p value	NS	0.02	NS	NS	NS	NS	NS	NS	NS	NS	NS	NS
5 FU-treated 4 wk (standard ringers)												
Mean	510.2	412.6	461.4	48.8	27.3	1E-1	7.3E-3	48.8	464.1	3.5E-4	2916.0	14.0
SE	12.2	6.7	8.9	4.2	2.3	7.7E-3	3.6E-3	4.2	9.2	7.4E-6	57.7	1.7
No.	11	11	11	11	11	11	11	11	11	11	11	11
p value	0.05	0.005	0.01	NS	NS	NS	NS	NS	0.01	0.02	0.02	NS

Legend same as in Table I.

mice treated for 4 wk with DMH or saline. Choline was substituted for sodium. The removal of sodium appears to unmask many of the characteristics observed at 14 or 20 wk.

Epithelial resistance, reactance, and phase angle were significantly decreased in DMH-treated mice under these conditions, however the elevation of the impedance locus and the characteristic capacitance increased significantly.

DISCUSSION

Although we have previously noted changes in sodium transport and transmural depolarization of the distal colon in this experimental model of colonic cancer, we have failed to demonstrate an alteration in the resistance of the bowel wall (16, 17). This may in part be explained by the observations made in these experiments which demonstrate that the surface epithelial resistance R_p decreased, whereas the resistance due to underlying muscle serosa or tight junctions may increase, resulting in no net change in resistance. The contribution of the tight junction or lateral intercellular space cannot be evaluated from this technique and would require impedance analysis in conjuction with intracellular recordings as has been previously described (18). The present technique represents the bowel wall as a simple lumped model (Fig. 4) rather than a complex or distributed model.

Since an increased influx of ions has been proposed as an early mitogenic signal (1, 2) during growth stimulation or transformation, the decrease in epithelial resistance suggests that an increase in the mucosal ionic conductance occurs after carcinogen treatment. This increase in ionic permeability is not solely due to an increase in sodium permeability since epithelial resistance was lower when sodium was removed from the bathing Ringer's solution

TABLE III
EPITHELIAL IMPEDANCE ANALYSIS CF_1 MOUSE DISTAL COLON

	R_0	R_∞	R_c	Reactance	R_p	Phase (ϕ)	x	r	F_c	T	w	Cap_c
	Ω	Ω	Ω	Ω	Ω · cm^{-2}	*rad*			*Hz*	*s*	*rad/s*	$\mu F \cdot cm^{-2}$
Control 14 wk (standard ringers)												
Mean	515.3	423.6	469.5	47.0	26.3	9.7E-2	1.1E-2	45.8	471.7	3.4E-4	2964.0	13.0
SE	6.5	5.7	5.8	1.8	1.0	4.2E-3	3.4E-3	2.0	5.8	4.2E-6	36.3	0.5
No.	13	13	13	12	12	13	13	13	13	13	13	12
DMH-treatment 14 wk (standard ringers)												
Mean	509.8	430.6	471.9	39.6	22.2	8.3E-2	4.2E-3	39.6	473.6	3.4E-4	2975.6	17.0
SE	8.7	4.6	6.1	2.7	1.5	5.1E-3	5.5E-3	2.7	6.2	4.4E-6	39.0	1.4
No.	12	12	12	12	12	12	11	12	12	12	12	11
p value	NS	NS	NS	0.025	0.025	0.025	0.02	0.05	NS	NS	NS	0.02

Legend same as in Table I.

TABLE IV
EPITHELIAL IMPEDANCE ANALYSIS CF_1 MOUSE DISTAL COLON

	R_0	R_∞	R_c	Reactance	R_p	Phase (ϕ)	x	r	F_c	T	w	Cap_c
	Ω	Ω	Ω	Ω	$\Omega \cdot cm^{-2}$	*rad*			*Hz*	*s*	*rad/s*	$\mu F \cdot cm^{-2}$
Control 4 wk (sodium-free ringers)												
Mean	592.8	515.8	559.2	43.5	24.4	7.7E-2	4.2E-3	43.5	561.0	2.9E-4	3524.9	12.0
SE	8.6	9.0	10.4	3.1	1.8	5E-3	4.9E-3	3.2	10.5	5.1E-6	65.9	0.9
No.	11	12	12	12	12	12	12	12	12	12	12	11
DMH-treated 4 wk (sodium-free ringers)												
Mean	639.0	564.9	598.8	34.0	19.0	5.7E-2	8.3E-3	34.0	599.8	2.6E-4	3768.9	15.0
SE	9.1	11.9	10.9	2.0	1.1	3.8E-3	3.7E-3	2.0	10.9	4.8E-6	68.4	0.8
No.	11	12	12	12	12	12	12	12	12	12	12	12
p value	0.005	0.005	0.02	0.02	0.02	0.005	0.02	0.02	0.02	0.02	0.02	0.05

Legend same as in Table I.

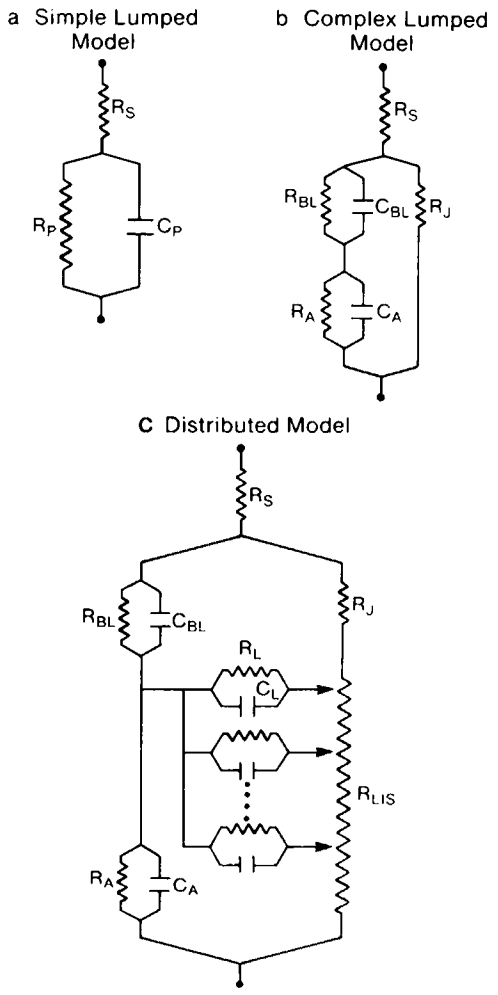

FIGURE 4 Circuit diagrams of the different representations that may be used to model the electrical behavior of an epithelium.

and replaced with choline in animals treated for just 4 wk with the carcinogen.

The fact that the resistance was significantly lower after only 4 wk of treatment is of considerable interest since changes in cell turnover as estimated by studies of thymidine labeling have not been observed until after at least 6 wk of carcinogen administration in this model (19), suggesting that these changes occur before an increase in proliferative activity can be detected by thymidine labeling techniques.

Whether this increase in ionic permeability represents a mitogenic signal of an obligate nature or is an associated but nonobligatory event in the malignant process cannot be determined from this study. It was noted however that the nonspecific cytotoxic agent 5-FU caused an increase in the epithelial resistance after only 4 wk of treatment, suggesting that the observed increase in ionic permeability was not due to nonspecific cytotoxic effects of the carcinogen.

The major drawback to measuring impedance at sequential frequencies is that it takes 10–15 min to obtain an impedance profile for a given piece of colon, during which time the resistance or capacitance may vary. Although these changes are small over the duration of the experiment, we have performed measurements at the same time in controls as in the carcinogen-treated group so that the observed differences do not represent time-dependent changes in impedance after the killing of the animal. Alternative methods of impedance analysis such as "square wave analysis," have been reported; "transient analysis" was reported 40 yr ago by Teorell (20). The advantage of this method is that all frequencies are measured simultaneously rather than sequentially so that an impedance profile may be obtained in <1 s. Unfortunately, one difficult aspect of this method is the inability to resolve the time constants from the individual RC elements that make up the circuit, particularly if the time constants are similar. Secondly, transient analysis is biased to the low frequencies since there are more of these frequencies represented in the applied square wave (21). Methods employing burst sine waves and pseudo-random binary

noise (22) allowing appropriate weighting of an entire frequency range may solve this problem. However, for this stable preparation in which we were more interested in differences between premalignant and benign colonic mucosa, simple sequential sinusoidal impedance analysis was accurate in demonstrating differences in the mucosa.

To our knowledge this is the first study employing epithelial impedance analysis in a model of cancer that demonstrates a change in the ionic conductance of the epithelium. Although we have previously reported a decrease in the electrical capacitance of the bowel wall at low frequencies (23), these observations have been extended to examine the changes in the circuit elements of the bowel, with particular attention to the surface epithelial cells where the large bowel cancer develops. Transepithelial electrical measurements outside the frequency domain have the disadvantage of measuring the electrical properties of the entire bowel wall, which may lead to overestimation of the electrical resistance of the true epithelium (24), especially since most stripped preparations are usually only partially stripped. Since the epithelial layer is usually impossible to separate from the underlying muscle, impedance analysis provides a technique to study the electrical properties of the true epithelial layer. Electrical changes were observed before electron or light microscopic evidence of dysplasia (data not shown), and impedance alterations appear to precede increases in cell turnover reported in this model (19).

In summary, impedance analysis is a simple and accurate technique which is able to detect changes in the ionic conductance of epithelia. It enables the components of a complex tissue to be resolved into their individual contributing parts. We have used this technique to examine the impedance profile of the colon in an animal model of large bowel cancer. A progressive increase in colonic ionic conductance appears to take place in the large bowel mucosa during the development of cancer. This technique is capable of identifying alterations in the electrical properties of the surface epithelium by a transepithelial approach which avoids the need for either intracellular recordings or a pure epithelial preparation.

APPENDIX I

The impedance measuring equipment used four electrodes constructed with silver and coated with silver chloride. Two working electrodes were used to excite the tissue, and readings were made with two measuring electrodes depicted in Fig. 1 (12, 16, 17). This configuration avoids electrode polarization, which may introduce errors into the impedance measurements. Fig. 1 depicts a programmable oscillator to the left of the circuit which is applied to a bridge transformer (26) which is interconnected through a switch network and bridge amplifier to apply the selected sine wave signal to the tissue. The oscillator will produce a signal in the measurement range of 10–10,000 Hz. The impedance measurement is a two-stage procedure. One side of the oscillating voltage signal from the bridge transformer (26) is applied to the working electrode (16), while the measuring electrode (17) is fed as one input to a differential amplifier (31). The other terminal of transformer (26) is connected to a common point of the parallel programmable resistance-capacitance arrangement identified as "R_1/C_1" in Fig. 1, and the other common point of which connects with electrical ground and the working electrode component of 12 (depicted as the plate with the continuous line). The measuring electrode of 12 (*broken line*) serves as the second input to the differential amplifier (31). The transformer's other terminal is connected to an additional amplifier (32). The gain of amplifiers 31 and 32 are the same, and their signal outputs feed into bridge amplifier (28) which is also a differential amplifier.

The first-stage measurement provides a first-order approximation of the tissue impedance which is the programmed value of R_1/C_1 when the bridge circuit is balanced.

At the completion of the first stage of the impedance measurement, a switch network excludes the tissue and a second set of programmable impedances, R_2/C_2, is substituted for the tissue. This second stage is depicted in the lower half of Fig. 1. One common point of R_2/C_2 is connected to the common ground of R_1/C_1 and the remaining common point of R_2/C_2 is fed into amplifier (31), the other input being grounded. R_2/C_2 is balanced against R_1/C_1 so that the current and voltage signals are the same. When comparison of the two signals yields a "zero error" the tissue impedance is equal to the final values of R_2/C_2. This two-stage procedure is performed at each of the frequencies of interest so that an impedance profile is obtained for the given tissue. The second stage of balancing R_2/C_2 against R_1/C_1 acts to neutralize distributed impedances associated with cabling, internal equipment, and circuit sources.

APPENDIX II

Fig. 5 depicts how the impedance profile is derived from the Nyquist plot. Values of resistance are obtained at frequencies varying between 10 and 10,000 Hz. These values are then plotted against the reactance using an iterative curve fit routine (Labtech Notebook, Laboratory Technologies Corp.

The reactance is derived from the capacitance using the formula reactance = $(1/2\pi fc)$, where f is the frequency in hertz and c is the capacitance in farads. The reactance is therefore the capacitive reactance. Having plotted the resistance against capacitive reactance, an inverted semicircle is obtained as shown in Fig. 5. This is depicted in an upright form (Cole plot) rather than in the conventional inverted form of the Nyquist plot to enable easier reading.

Using the simple lumped model (Fig. 4 *a*) to represent the circuit components that make up the colon, the impedance (Z) can be written in complex notation as:

$$Z = R_s + \frac{R_p/jwC_p}{R_p + 1/jwC_p}, \qquad \text{(A1)}$$

where j is the complex operator $\sqrt{-1}$, R_s is the series resistance, R_p is the epithelial resistance, C_p is the epithelial capacitance, and w is the angular

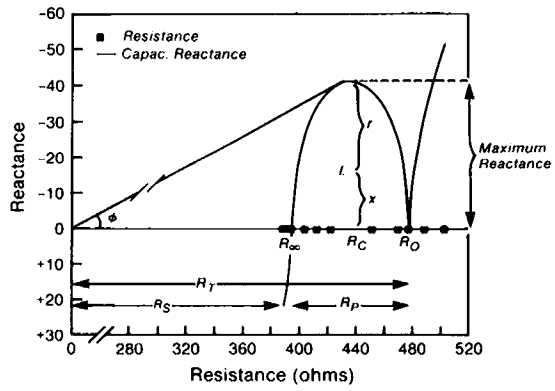

FIGURE 5 Illustration of the impedance profile and how the various circuit parameters are derived. This is discussed in Appendix II.

frequency. Separating real and imaginary parts:

$$Z = R_s + \frac{R_p}{1 + w^2C_p^2R_p^2} - j\frac{wC_pR_p^2}{1 + w^2C_p^2R_p^2}. \quad \text{(A2)}$$

In Fig. 5

$$R_o = R_p + R_s = R_t \quad \text{(A3)}$$

and

$$R_\infty = R_s, \quad \text{(A4)}$$

where R_o and R_∞ are the tissue resistance at 0 and infinite frequency, respectively. R_t is the total resistance of the tissue. R_pC_p may be represented as the time constant T and Eq. A2 may be rewritten as:

$$Z = \left(R_\infty + \frac{R_o - R_\infty}{1 + w^2T^2}\right) - j\left[\frac{wT(R_o - R_\infty)}{1 + w^2T^2}\right]. \quad \text{(A5)}$$

In this equation the first term in parentheses is the real component R (resistance) of the colon impedance and the second term in the brackets represents the reactance (reactive capacitance) in the xy plane. Real and reactive terms are functions of w and thus z is also. When frequency is changed between o and ∞, z will change continually along the curve in the xy plane of the graph (Fig. 5). This curve is a perfect semicircle, although for the purpose of illustrating the calculations it has been distorted in Fig. 5 and is known as an impedance plot.

From Eq. A5 it follows that:

$$R = R_\infty + \frac{R_o - R_\infty}{1 + w^2T^2} \quad \text{(A6)}$$

and

$$\text{reactance} = -\frac{wT(R_o - R_\infty)}{1 + w^2T^2}. \quad \text{(A7)}$$

R and reactance can be considered as functions of the parameter wt, and are related to z by:

$$Z = (R^2 + \text{reactance}^2)^{1/2} \quad \text{(A8)}$$

and to the phase angle ϕ by the relationship:

$$\tan\phi = \frac{\text{reactance}}{R}. \quad \text{(A9)}$$

Elimination of wT from Eqs. A6 and A7 yields the expression for the impedance plot in the xy plane of Fig. 5:

$$\text{reactance} = \frac{(R_o - R_\infty)\,[(R_o - R)/(R - R_\infty)]^{1/2}}{(R_o - R_\infty)/(R - R_\infty)}. \quad \text{(A10)}$$

This equation was used in the curve fit program to derive R_o and R_∞. The maximum reactance was derived from the plot and is defined as the maximum capacitive reactance of the tissue. Eq. A10 is the analytic expression for the impedance plot and represents a circle with the impedance locus (center of the circle) close to the x-axis (Fig. 5).

$$R_c = (R_o + R_\infty)/2 \quad \text{(A11)}$$

and R_c is defined as the characteristic resistance for the colon and lies on the x-axis midway between R_o and R_∞. The center was often slightly elevated or suppressed from the x-axis and this value x was derived from

$$X = \frac{(1/2\,R_p)^2 - (\text{maximum reactance})^2}{2(\text{maximum reactance})} \text{ (Pythagoras).} \quad \text{(A12)}$$

The radius (r) of the impedance plot was then derived from

$$r = x + \text{maximum reactance.} \quad \text{(A13)}$$

The characteristic frequency (F_c) was derived from

$$F_c = \text{arc tangent}\,\frac{(\text{maximum reactance})}{R_c} \quad \text{(A14)}$$

and is defined as the frequency at which the capacitive reactance is maximum and coincides with R_c. T, the time constant for the colon, was derived from

$$T = R_pC_p. \quad \text{(A15)}$$

The angular frequency w was derived from

$$w = \frac{1}{T} \quad \text{(A16)}$$

and the characteristic capacitance (C_p) was derived from

$$C_p = \frac{1}{2\pi F_c R_p}. \quad \text{(A17)}$$

S. Pesavento provided secretarial help in the preparation of this manuscript.

This study was supported in part by the Veteran's Administration and a grant from American Mediscan Inc., Los Angeles.

Received for publication 30 March 1987 and in final form 16 July 1987.

REFERENCES

1. Rozengurt, E. 1986. Early signals in the mitogenic response. *Science (Wash. DC).* 234:161–166.
2. Singer, S. J. 1985. On the transduction of signals at the cell surface. *In* Cell Membranes and Cancer. T. Galeotti, A. Cittadini, G. Neri, S. Papa, and L. A. Smets, editors. Elsevier North-Holland, Inc., New York. 1–10.
3. Schlessinger, J. 1980. The mechanism and role of hormone induced clustering of membrane receptors. *Trends Biochem. Sci.* 5:210–214.
4. Schecter, Y., L. Hernaez, J. Schlessinger, and P. Cuatrecasas. 1979. Epidermal growth factor: biological activity requires persistent occupation of high-affinity cell surface receptors. *Nature (Lond.).* 278:835–838.
5. Schreiber, A. B., T. A. Libermann, I. Lax, Y. Yarden, and J. Schlessinger. 1983. Biological role of epidermal growth factor receptor clustering: investigation with monoclonal antibodies. *J. Biol. Chem.* 258:846–853.
6. Moolenaar, W. H., L. G. J. Tertoolen, R. Y. Tsien, P. T. Van der Saag, and S. W. De Laat. 1983. Na^+/H^+ exchange: cytoplasmic pH and the action of growth factors in human fibroblasts. *J. Biol. Chem.* 259:8066–8069.
7. Paris, S., and J. Pouyssegur. 1984. Growth factors activate the Na^+/H^+ antiporter in quiescent fibroblasts by increasing its affinity for intracellular H^+. *J. Biol. Chem.* 259:10989–10994.
8. Leffert, H. L., and K. S. Koch. 1982. Monovalent cations and the control of hepatocyte proliferation in chemically defined medium. *In* Ions, Cell Proliferation, and Cancer. A. L. Boynton, W. L. McKeehan, and J. F. Whittfield, editors. Academic Press, Inc., New York. 103–130.
9. Metzger, H. 1977. Receptors and Recognition. Series A. P. Cuatrecasas and M. F. Greaves, editors. John Wiley & Sons, Inc., New York. 4:74–102.

10. Filipe, M. I. 1975. Mucous secretions in rat colonic mucosa during carcinogenesis induced by dimethylhydrazine. A morphological and histochemical study. *Br. J. Cancer.* 32:60–64.
11. Oplatka, A., J. E. Friedman, and K. Rosenheck. 1985. Reorganization of the cytoskeleton in transformed and tumor cells may be intimately coupled with changes in ion transport through the plasma membrane. *In* Cell Membranes and Cancer. T. Galeotti, A Cittadini, G. Neri, S. Papa, and L. A. Smets, editors. Elsevier North-Holland, Inc., New York. 117–123.
12. Statistics of the American Cancer Society 1987. *CA Cancer J. for Clin.* 37:2–19.
13. Schultz, S. G. 1981. Homocellular regulatory mechanisms in sodium-transporting epithelia: avoidance of extinction by flush-through. *Am. J. Physiol.* 10:F579–F590.
14. Cole, K. S. 1972. Membranes, Ions and Impulses. University of California Press, Berkley, CA. 12.
15. Davson, H. 1964. A Textbook of General Physiology. Little, Brown & Co. Inc., Boston. 15:681.
16. Davies, R. J., W. F. Weidema, L. Palmer, and J. J. DeCosse. 1983. Increased sodium absorption by the distal colon in 1,2-dimethylhydrazine-treated Sprague-Dawley rat. *Surg. Forum.* 34:183–185.
17. Goller, D. A., W. F. Weidema, and R. J. Davies. 1986. Transmural electrical potential difference as an early marker in colon cancer. *Arch. Surg.* 121:345–350.
18. Kottra, G., and E. Fromter. 1984. Rapid determination of intraepithelial resistance barriers by alternating current spectroscopy. *Pfluegers Arch. Eur. J. Physiol.* 402:409–420.
19. Deschner, E. E. 1978. Early proliferative defects induced by six weekly injections 1,2-dimethylhydrazine in epithelial cells of mouse distal colon. *Z. Krebsforsch.* 91:205–216.
20. Teorell, T. 1946. Application of square wave analysis to bioelectric studies. *Acta. Physiol. Scand.* 12:235–254.
21. Diamond, J. M., and T. E. Machen. 1983. Impedance analysis in epithelia and the problem of gastric acid secretion. *J. Membr. Biol.* 72:17–41.
22. Clausen, C., and J. M. Fernandez. 1981. A low-cost method for rapid transfer function measurements with direct application to biological impedance analysis. *Pfluegers Arch. Eur. J. Physiol.* 390:290–295.
23. Davies, R. J., R. D. Juncosa, D. Kapland, C. Pempinello, H. Asbun, and Y. H. Pilch. 1986. Colonic epithelial impedance analysis in a murine model of large-bowel cancer. *Arch. Surg.* 121:1253–1258.
24. Fromm, M., J. Schulzke, and U. Hegel. 1985. Epithelial and subepithelial contributions to transmural electrical resistance of intact rat jejunum in vitro. *Pfluegers Arch. Eur. J. Physiol.* 405:400–402.